

Processing parameters optimization for thermochemical writing of DOEs on chromium films

V. V. Cherkashin, E. G. Churin, V. P. Korol'kov, V. P. Koronkevich, A. A. Kharissov, and A. G. Poleshchuk
Institute of Automation and Electrometry, Russian Academy of Sciences 630090, Novosibirsk, Russia

J. H. Burge
Steward Observatory, University of Arizona, Tucson, AZ

ABSTRACT

Computer-generated holograms are limited by conventional lithographic fabrication capabilities which rely on accurate deposition, exposure, and developing of photosensitive chemicals. We present an alternate fabrication technology that uses a focused laser beam to write patterns by inducing a thermochemical change in a bare metal film. The patterns are developed using a single etching step that dissolves the non-exposed metal. The thermochemical writing method allows holograms to be directly written onto large-diameter, thick, and non-flat substrates, requiring no intermediate steps that compromise the ultimate accuracy. Circular patterns for optical testing were written using a polar-coordinate laser writer. The laser power and control requirements are shown to be modest and the etching is shown to be tolerant of temperature and concentration variations. The technology is demonstrated with the fabrication of CGH's up to 136 mm in diameter used for optical testing.

Keywords: laser writing, computer-generated holograms, circular laser writing, optical testing of aspheres.

1. INTRODUCTION

Computer-generated holograms are commonly fabricated using lithographic techniques developed for VLSI chip fabrication. The patterns are written using Cartesian coordinate optical or electron beam writers to expose thin films of photosensitive chemicals, or photoresists, that are deposited onto glass substrates. After developing, these images are transferred to a metal film, typically chromium. The chrome pattern can be used directly, or it can act as a mask for replicating the pattern, or for etching the glass substrate. These methods work quite well for the electronics industry where the patterns are generally described as horizontal and vertical lines and the substrates are nominally flat, a few millimeters thick, and less than 150-200 mm across. We present improvements in the equipment and techniques for fabricating large diffractive optics.

Since many applications for diffractive optics use holograms made of circularly symmetric rings, these patterns are optimally generated using polar-coordinate pattern generators. These machines use continuous rotation of the substrate while the writing beam is moved accurately in the radial direction. Several such machines have been developed for writing ¹into resist with focused laser beams^{1,2} and electron beams³. The work in this paper was performed using a circular laser writing system built at the IAE that is capable of writing patterns up to 30 cm in diameter with accuracy of 0.1 μm .^{4,5} (This machine is also capable of writing general non-circular patterns by using polar coordinate transformation software with an accurate rotary encoder and computer-controlled amplitude modulation of the laser beam.)

The limitations from depositing and developing photoresists on non-standard substrates are avoided by using another fabrication method — thermochemical writing. The thermochemical technique avoids the difficulties of applying and controlling photoresist by writing the latent image directly onto a chrome coated substrate using a laser beam. (See Fig. 1.) The power absorbed by the laser heats the surface and the increased temperature causes an oxide layer to form.⁶ The dynamics of the laser writing are chosen to build up enough oxide where the laser had scanned with minimal thermal

email: VVC- cherkashin@iae.nsk.su; EGC- churin@iae.nsk.su; VPK- korolkov@iae.nsk.su; JHB- jburge@as.arizona.edu

broadening. After it is exposed, the pattern is developed by immersing in a caustic bath that dissolves the bare chrome much more quickly than the chrome oxide. So after developing, a pattern of chrome remains where the laser had exposed the surface and created the oxide layer.

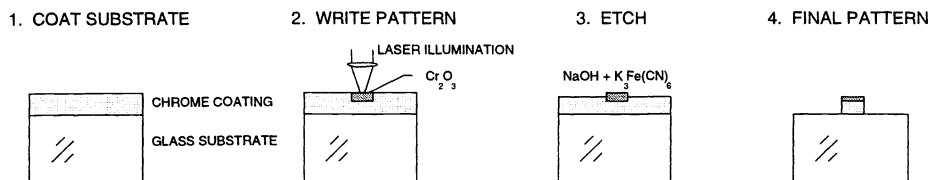


Figure 1. Pattern generation using thermochemical technique.

The thermochemical writing method described in this paper provides a simpler technique for mask and CGH production that eliminates some difficulties and fabrication errors that are connected with the use of resists. The critical parameters for the thermochemical writing technology are explored. The laser power requirements are given for writing into chrome films of 50 and 80 nm thickness, with varying writing velocity. The selectivity of the etching is shown to be insensitive to changes in temperature and concentration, and the etching rate is shown to depend strongly on these parameters. We discuss processing parameters optimization for minimizing fabrication errors for writing large holograms for optical testing. These patterns, up to 136 mm in diameter and with features as small as 0.65 μm , were interferometrically measured and shown to be of excellent quality.

2. DIFFRACTIVE ELEMENTS FOR OPTICAL TESTING

Optical testing of aspheric surfaces using computer-generated holograms (CGH) has proven to be a powerful and economical technique. Computer-generated holograms are readily designed to create wavefronts for testing arbitrary optical surfaces and systems. Circular holograms (zone plates) have been used in numerous configurations for measuring aspheric surfaces.⁷⁸⁹¹⁰ One important application of binary computer-generated holograms is for certification of null correctors used to measure concave aspheres. This test avoids the type problem that afflicted the Hubble Space Telescope — fabricating an expensive primary mirror to the wrong shape due to an error in the null corrector. The CGH test has been used to verify the optical tests of 3.5-m primary mirrors to $\lambda/100$ ¹¹, and has been implemented for a 6.5-m $f/1.25$ primary mirror¹². Another important application of circular holograms is the use of CGH test plates for measuring convex aspheric surfaces.¹³ These holograms are fabricated exclusively by thermochemical writing because they are large and must be written onto steeply curved substrates. This test has been successfully implemented using holograms up to 1.2-m in diameter.¹⁴

The tests for the large, fast primary mirrors require large holograms that may not be feasible using conventional lithographic techniques. For example, testing of the 6.5-m primary mirrors for MMT and Magellan telescopes required the 136 mm diameter hologram that has 38,000 and testing of the 8.4-m primary mirrors for the Large Binocular Telescope requires a 208 mm diameter hologram with 64,000 rings. The physical size of the holograms and the large amount of data required to write these circular patterns using a x-y writers are prohibitive. These holograms are unique optics, only one is required with a given prescription, and they must be assured to be of high quality. To achieve the required test accuracy, the holograms require patterns with absolute ring position accuracy of 0.2 μm and surface figure of $\lambda/10$.¹⁵

3. LASER WRITING SYSTEM

The investigation of technology for CGH fabrication was made using a new version of the laser writing system built at the Institute of Automation and Electrometry.⁴ The circular laser writing system is shown in Fig. 2 and the specifications for writing typical holograms are given in Table 1. The substrate with thin chromium film (1) is fixed on the top of precision air-bearing spindle. Laser power for a 1-W argon laser (2) is controlled with 10-bit resolution using a closed loop servo that uses a photodiode (5) for detection and an acoustooptical modulator (4) for control. The writing beam is focused to a 0.8 μm spot and the focus is held by servo control. The focusing optical system (6) is moved radially using an air bearing stage (7), linear motor (8), and interferometric position feedback (9). The range of stage displacement is 250 mm, the positioning precision is near 50 nm rms, and the positioning resolution is 10 nm.

Table 1. Typical parameters for writing a pattern.

Substrate rotation speed	number of pulses of angular raster per one revolution	recorded line width	radial step	substrate diameter	substrate thickness
600-rpm	1602000	0.6 - 1.2 μm (controlled by beam intensity)	0.1 - 0.7 μm	20-300 mm	1.5-30 mm
850 rpm	1134000				

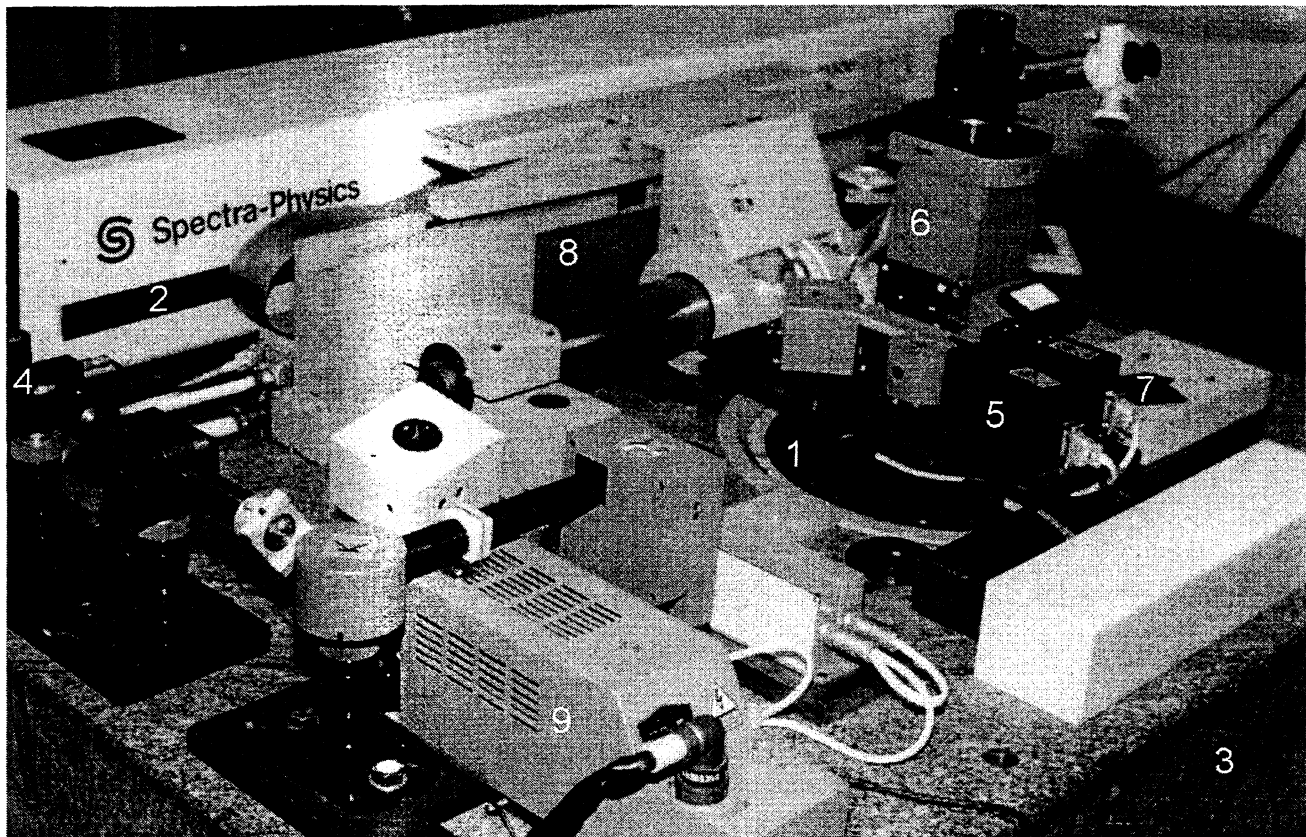


Figure 2. Circular laser writing system at the IAE.

Circular ring patterns are written by exposing each of the inner and outer edges with 1 rotation and filling the middle with a spiral pattern. More general patterns are written using coordinate transform software to define the patterns in cylindrical coordinates, then accurately synchronizing laser pulses with angular position to expose pixels on the surface. The spatial resolution for linear features using the polar coordinate writer is demonstrated below in Fig. 3.

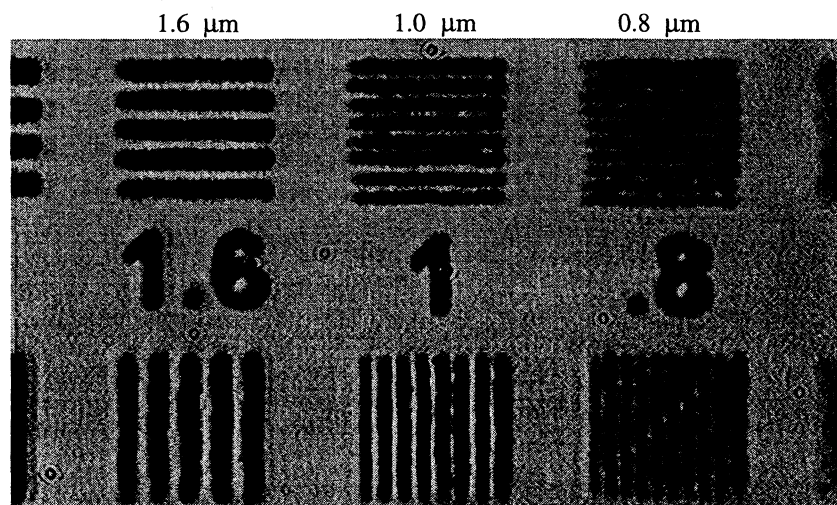


Figure 3. Spatial resolution test pattern with 1.6, 1.0 and 0.8 μm line spacing, written on 80 nm sputtered chromium film with using thermochemical technology

4. LASER THERMOCHEMICAL TECHNOLOGY

It has been shown that thermal action of laser radiation in an oxidative environment activates an oxidation reaction on the surface and in the volume of thin metal films. Laser heating of chromium films causes build-up of the thin oxide layer which is stable in some chromium etchants.¹⁶ This effect allows the direct generation of patterns with spatial resolution better than 1000 line/mm onto bare chrome films. The most critical steps are the laser exposure and the etching. The physical phenomena connected with these issues are studied in detail below.

The main shortcomings of thermochemical writing in comparison with writing on resist films are less (about 10 times) light sensitivity and considerable dependence of recorded line width on the light power and exposing time (or scanning velocity). However, these problems are overcome with accurate computer control of the laser power and careful calibration.

4.1 Fabrication of chrome films

The thermochemical recording uses an inorganic material, a thin metal film (chromium) instead of the photosensitive film used in conventional lithography. The chromium mask is formed on the CGH substrate directly. The chromium film is the optimum material for amplitude hologram and mask production because of its hardness, high radiation absorption, and excellent adhesion to glass substrates. The technologies for chromium film deposition and processing in various etchants have been developed over many years by the microelectronics industry.

Selection of film thickness depends on the application of the written structure (photomask or reflective binary DOE), required spatial resolution, and fabrication constraints. The quality of the chrome coating affects the thermochemical writing. Experiments have shown that the image formation takes place for chromium films from any deposition method. However, the best results in terms of resolution were achieved for films deposited by RF-sputtering in an Ar atmosphere. Spatial resolution of writing on sputtered Cr films reaches 1500 lines/mm. The high density results in smooth boundaries of pattern features and absence of crystal generation, but requires approximately twice as much power in the writing beam. The coatings for the very large holograms must be deposited by evaporation to achieve good uniformity. The evaporated films give somewhat worse spatial resolution than the sputtered films, 700-1000 lines/mm. However the thermochemical writing on such films is accompanied by considerable alteration of reflection (up to several percent), and that permits to control writing process before etching.

4.2. Writing method

The IAE writing system was used to expose chromium films for a set of experiments. The recording spot was approximately 0.7 μm in diameter with velocity that was varied from 4.4 to 175 cm/s. It corresponds to radii of 0.7 mm to 28 mm at rotation speed 10 cycles/sec. The optimum power for thermochemical writing was within 10 - 30 mW for this velocity range and focusing 40X objective with N.A.=0.65. The exposed films were developed in the etchant consisting of 6 parts of 25% solution of $\text{K}_3\text{Fe}(\text{CN})_6$ and 1 part of 25% solution of NaOH. For experiments we used chrome coated glass substrates of Robotron GmbH (sputtered films with thickness of 65 nm) and 80 nm thick vapour-deposited films on glass substrates. For hologram writing we used 80 nm thick evaporated films on fused silica substrates. The evaporated films demonstrate the same behaviour for glass and fused silica substrates. But for higher power was required for writing on the fused silica substrates because of the higher thermal conductivity of fused silica.

Since the most narrow diffractive zones of circular hologram are written not less than in 3 passes on the same radius. (It is necessary to average radial error and decrease influence of the number of passes, as will be explained in more detailed below) Figure 4 shows some test patterns recorded by triple passes on the chromium films fabricated by sputtering and vapor deposition. For the 1 μm

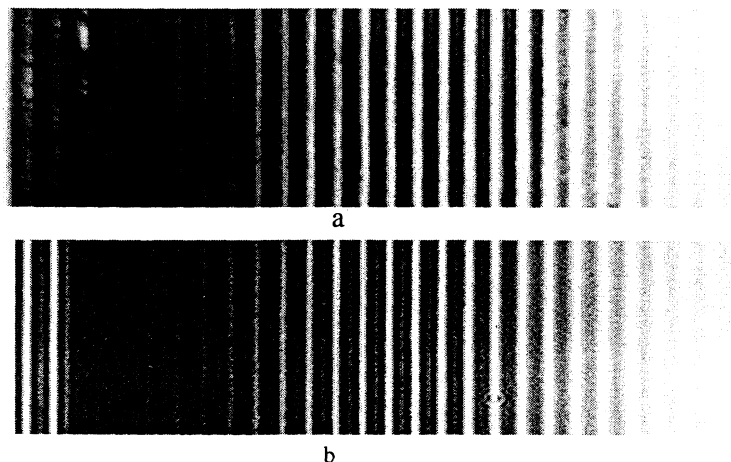


Figure 4. Microphotographs of patterns showing effect of laser beam power variation for a) evaporated and b) sputtered films. The line spacing is 1.5 μm . The power decreases from left to right, leaving faint, under-exposed lines on the far right.

features, the two coatings have excellent performance, but the sputtered coating gives a little better definition. The width of recorded lines is seen to depend linearly on the light power. This effect is shown quantitatively for both evaporated and sputtered films in Fig. 5, which shows the measured line width varying linearly with laser power for different spot velocities. Laser beam power was normalized to maximum required power for maximum linear velocity for convenient comparison.

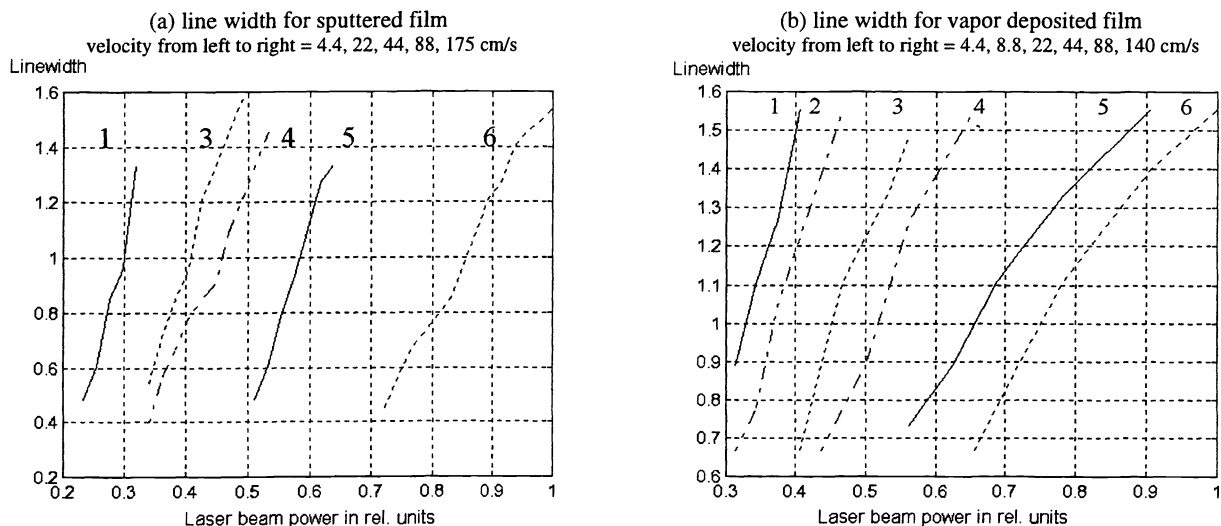


Figure 5. Measured line width in μm as a function of laser beam power for several linear velocities for (a) 65 nm thick sputtered Cr film and (b) 80 nm thick evaporated Cr film.

For recording lines of constant width, there exists a non-linear relationship between the laser power and the velocity of the writing spot over the substrate. The velocity dependence of the power for writing 1.2- μm and 0.7- μm lines recorded by triple passes are shown in Fig. 6 for sputtered and evaporated films. The tendency to saturation after 20 cm/s allows us to avoid a large range of laser beam power control even though we use a large variation in velocity. It is interesting that k , the ratio of power for 0.7 μm lines to that for 1.2 μm lines ($k = P_{0.7}/P_{1.2}$) is approximately constant (considering measurement error). For the sputtered film this ratio is more narrow, which characterizes the increased sensitivity of thermochemical writing to laser beam power for evaporated films.

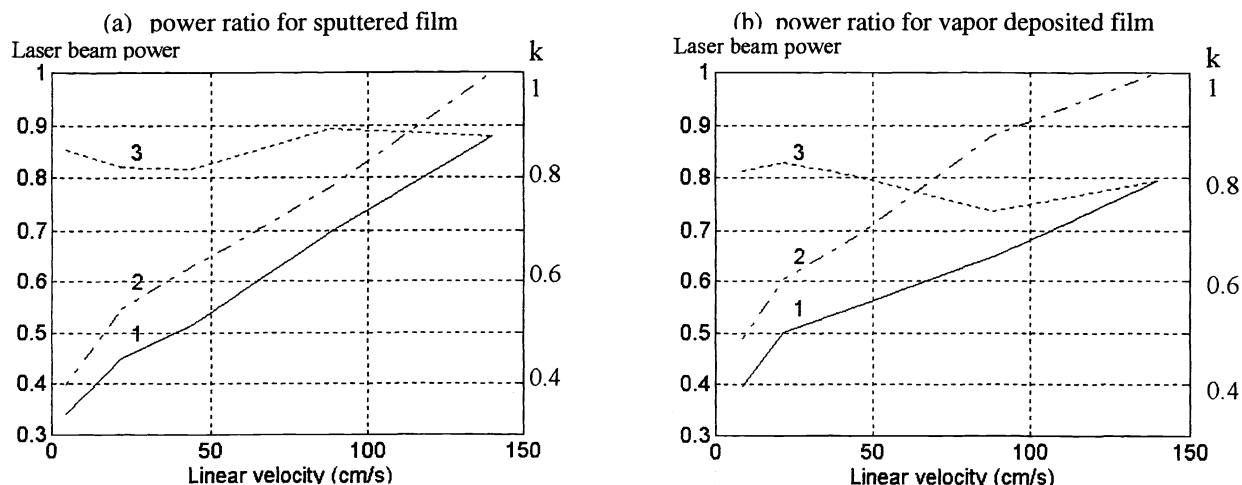


Figure 6. The range of normalized laser beam power for thermochemical writing (1) for 0.7 μm wide lines, (2) for 1.2 μm wide lines. The ratio of power for 0.7 μm lines to that for 1.2 μm lines is shown as curve (3).

Variation of the linear velocity of the writing laser beam can be changed by nearly 2 orders of magnitude for writing with the circular laser writing system. To control laser beam power with this dynamic range for writing on photoresist would be difficult. The thermochemical writing technique requires the power to change by only a factor of 2.5 for velocity changes of 30 times.

As described above, the final line width is controlled by writing the inside and outside edges of the ring and filling in the rest with a spiral pattern. Accurate lines require careful control and characterization of the writing power. To evaluate this sensitivity we wrote tests with 2 extreme situation: with total overlap (spacing equal to 0 for 3 passes) and no overlap (single pass). The ratio of triple pass line width to single pass line width at the same laser beam power as function of linear velocity is shown in Fig. 7. Evaporated films are more sensitive to spacing; the curve for 0.7 μm is only conditionally because these lines are poorly defined. This figure shows that using wider lines is preferable for accurate hologram writing. It is explained that fine lines are written by the peak of temperature distribution induced by the laser beam and writing near this threshold is sensitive to any variation of parameters. It also shows that writing of high numerical aperture holograms with narrow diffractive zones requires calibration of writing onto the actual coatings.

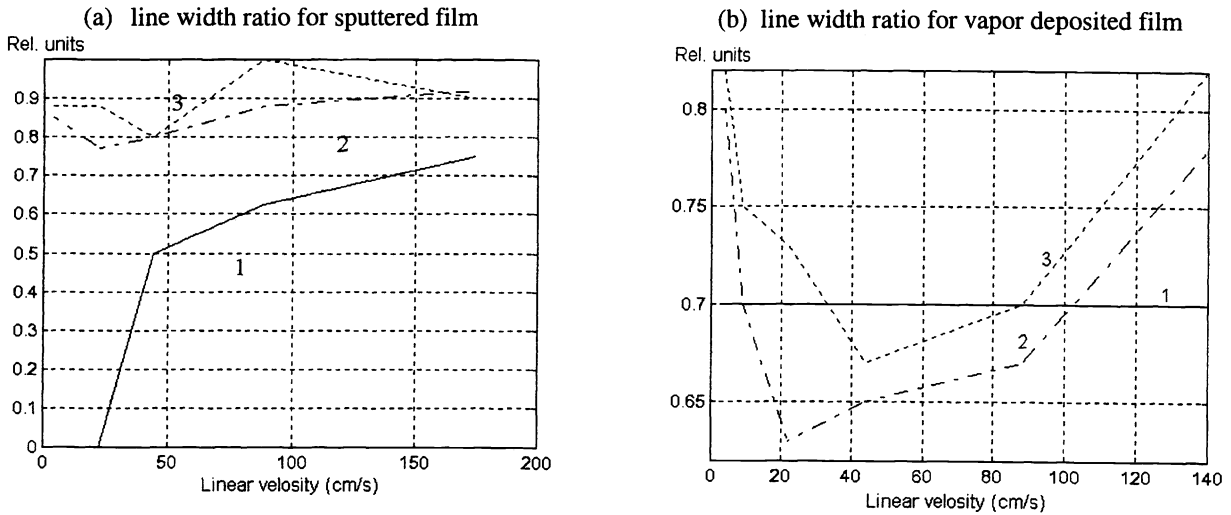


Figure 7. Ratio of measured line width for triple-pass and single-pass writing at fixed laser power, as function of linear velocity for triple-pass line width of (1) 0.7 μm , (2) 1.0 μm , and (3) 1.2 μm .

We also explored the sensitivity of thermochemical writing to variation in the etching time. Figure 8 shows how the line width for the final pattern can be degraded by etching too long. The measured line widths are shown for rings written at 100 cm/s for triple-pass exposures as a function of relative etching time. The etching time is normalized to one for complete dissolution of the same unexposed film. Evaporated films are shown to be less sensitive to over-etching, especially for 1 μm lines.

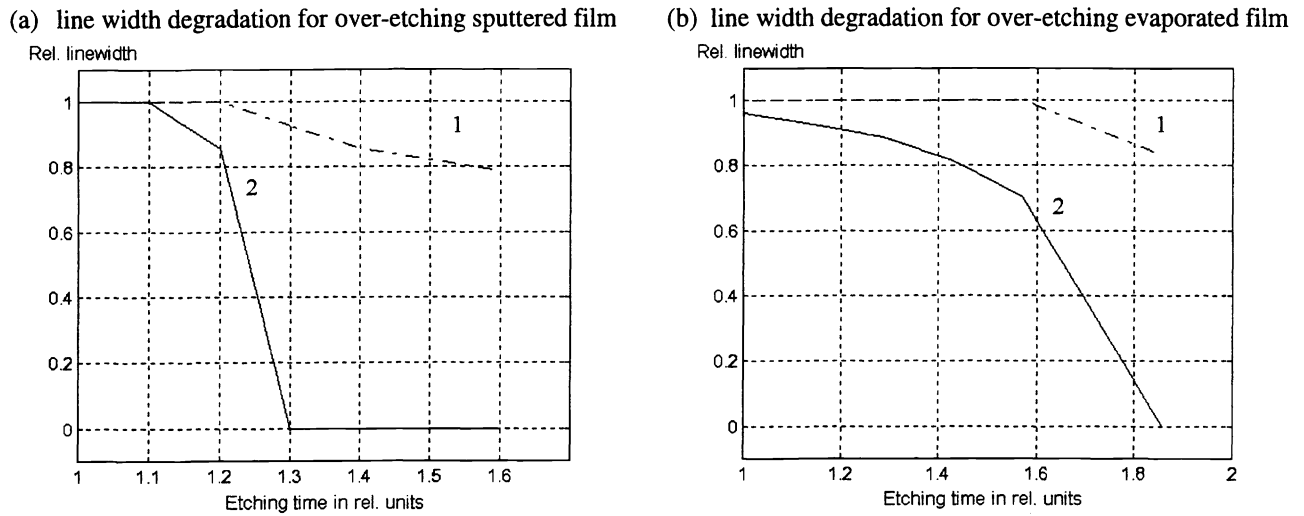


Figure 8. Degradation of line width with over-etching. The curves show the measured line width for exposures at 100 cm/s as function of relative etching time for initial line width of (1) 1 μm and (2) 0.7 μm . The etching time is normalized to one for complete etching of the unexposed film.

4.3. Writing algorithm for axial symmetrical CGHs.

Application of thermochemical technology of laser writing to fabrication of high-precision computer-generated holograms for optical testing requires high stability of the writing algorithm to errors in processing parameters and in the writing system. Greatest contribution to total error is made by radial shift of the lines, which directly causes a phase error in the wavefront, thus an error in the surface measurement. Errors in line width are less important since they affect primarily diffractive efficiency and not phase. However, irregular duty cycle is nevertheless undesirable in view of increasing diffusion of light. In order to reduce amount of irregular duty cycle transitions between zones made different number of beam tracks the minimal number of beam tracks in zone has been selected equal to 3. At thrice-repeated track on the same radius the spatial resolution maintains acceptable level near 700 lines/mm, and the errors of radial coordinate positioning are averaged. In particular this error is more important for narrow zones.

The method of exposing zones is shown in Fig. 9. Increasing zone width is accompanied by expanding the distance between the inside and outside tracks as long as the consecutive passes overlap without gaps. The gaps can appear because of radial positioning error or writing beam power selection. If these tracks are close together, the space between is filled by making a single pass. For wide lines, the space between these passes is filled by executing a spiral pattern from the outside edge to the inside.

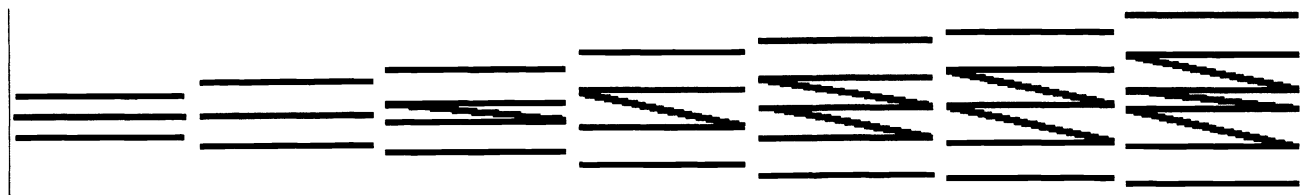


Figure 9 The method of ring zone exposure.

Dependence of beam power on radial position is defined by making small exposures onto the same substrate. The test exposures consist of small DOE fragments on different radii at diverse power levels.

4.4 Selective etching

The preliminary investigations of a number of the chromium etchants consisting of HCl, mixture of $\text{Ce}(\text{SO})_4$ and HNO_3 , mixture of $\text{K}_3\text{Fe}(\text{CN})_6$ and KOH , $\text{K}_3\text{Fe}(\text{CN})_6$ and NaOH showed that the most suitable etchant is the last one. Other etchants either have insufficient selectivity (contrast) or their reaction with chromium is very violent and requires a catalyst. The etchant studied was made from a 25% ($N=0.25$) solution of $\text{K}_3\text{Fe}(\text{CN})_6$ and a 25% solution of NaOH . Higher concentration could not be used because the $\text{K}_3\text{Fe}(\text{CN})_6$ solution saturates at 30% at 20°C .

The etching was monitored by measuring the optical transmittance of the chrome film during the etching process, using the device shown in Fig. 10. A light source with collimating objective illuminates the cuvette with the etchant. The investigated samples (one with exposed and one with unexposed films) are placed in front of the opaque screen which has three holes for limiting scattered light. The central hole is used for the normalization. The objective O2 forms the images of these holes on the surface of the photodiodes PD1, PD2, PD3. The output signals (u_1 , u_2 , u_3) from these photodiodes are digitized and stored on computer. The etchant temperature is measured using a thermoresistor and controlled by a heater H and cooler.

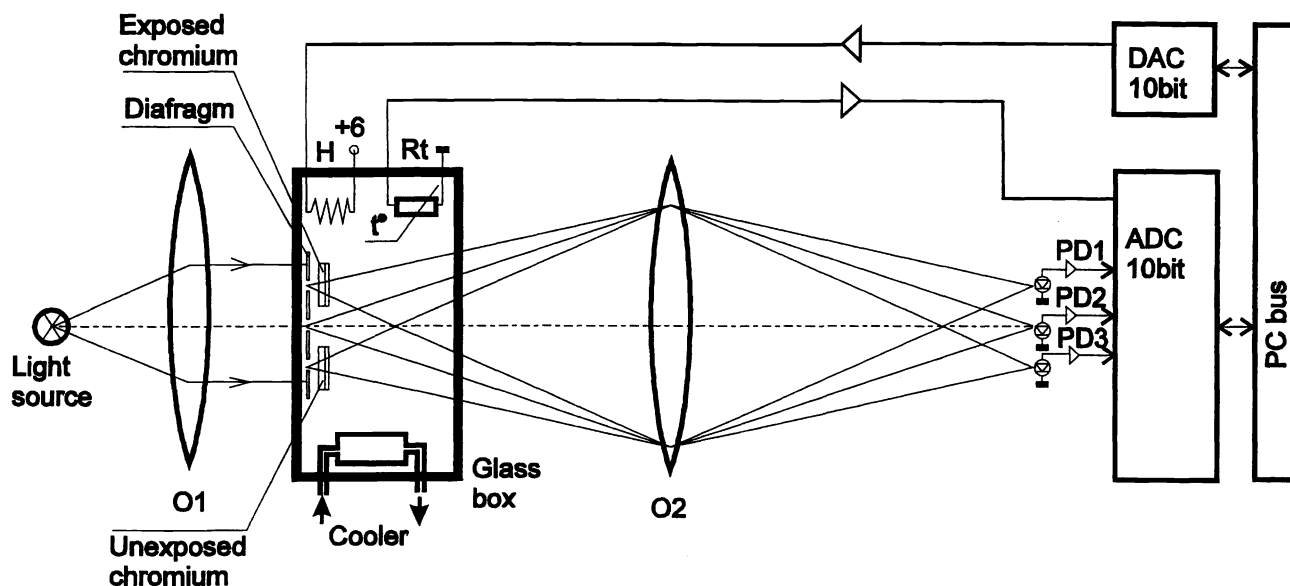


Figure 10. Schematic diagram of apparatus used for etching experiments.

Typical curves of the etch process are shown in Fig. 11 -- the left curve corresponds to the unexposed film and the right curve to the optimally exposed one. These curves show two effects, a surface effect and a change in the bulk chromium. The lag is due to the surface layer of chrome oxide. As the oxide layer is being slowly dissolved, the transmission does not change. Since the exposed chrome has more oxide than the native layer on the unexposed metal, the exposed chrome is protected longer. After the oxide is dissolved, the etching rate of the chrome is seen to be slower for the exposed metal, seen in the plots as a difference in slope. This is due to a thermochemical change in the chromium. This may be annealing of the chrome, making it more resistant to chemical attack.

We measured the time when transmission becomes equal to 0.5, which corresponds to the film thickness of about 8 nm. Dividing the etched thickness by this time we get the average etching rate. The selectivity coefficient K is defined as a ratio of the average etching rates for unexposed and exposed films. Figure 12 shows how the etching rate for unexposed film and the selectivity coefficient depend on volume fraction M of the NaOH solution. Using this curve, we chose $M = 0.14$ for the working etchant to be used in all further experiments. This is made by mixing 6 volume parts of 25 % solution of $\text{K}_3\text{Fe}(\text{CN})_6$ and 1 part of 25% solution of NaOH .

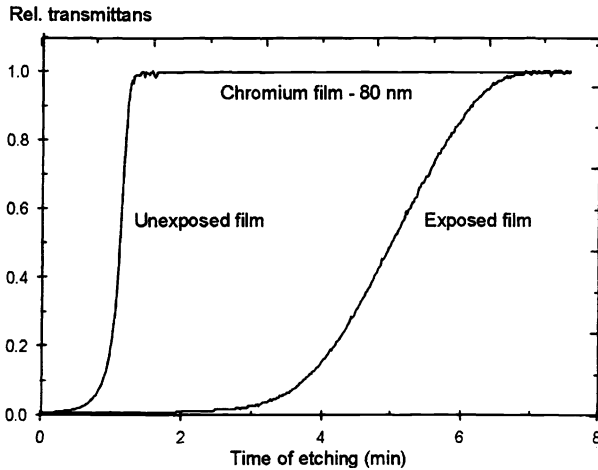


Figure 11. Characteristic etching curves for 80 nm Cr films showing the optical transmittance vs. time during etching.

We used the above apparatus to measure the dependence of etching rate and selectivity on concentration and temperature. As the temperature was varied from 17° C to 28° C, the etching rate increased linearly. However, the selectivity, which is the critical parameter for thermochemical writing, remained constant.

The developing time for this etchant was about 2 minutes for chromium film thickness of 50 - 80 nm. This is very short time for developing very large substrates covered by chromium films. With the purpose of increasing the developing time we diminished the etchant concentration N (defined as the weight of dissolved materials divided by the weight of solution) by diluting of 1 milliliter of 25% etchant with W milliliters of water. In this case we have $N_0 = 0.25 \cdot \rho_0 / (\rho_0 + W)$, where $\rho_0 = 1.16$ is the density of initial etchant. The curves $V(N)$ and $K(N)$ are shown on Fig. 13.

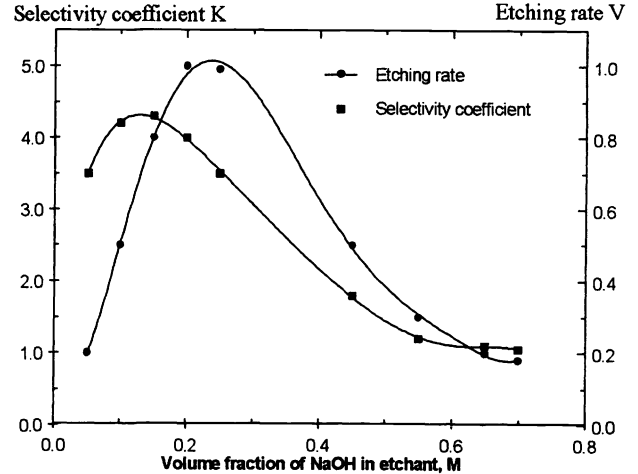


Figure 12. Dependence of etching velocity V and selectivity coefficient K on volume fraction of the 25% NaOH solution at 22°C.

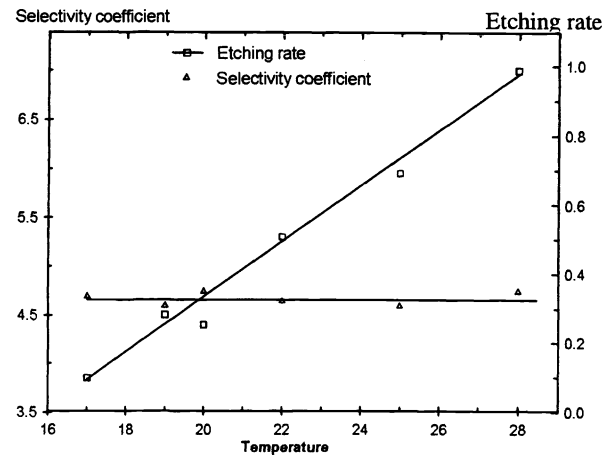


Figure 13. Dependence of etching rate and selectivity on temperature.

5. FABRICATION AND MEASUREMENT OF DOE'S

The writing techniques described above and thermochemical technology were used to fabricate binary DOE's that were evaluated interferometrically. The chrome patterns were direct-written onto flat substrates and used without any further processing in reflection. The patterns were designed to reflect spherical wavefronts so they can be accurately evaluated. The diffracted wavefronts were measured with a phase-shifting Fizeau interferometer.

A 58-mm $f/1.1$ zone plate was fabricated directly into the 100 nm chromium film on a flat fused silica substrate. The hologram was designed for $\lambda = 632.8$ nm wavelength and had 9879 rings, with spacing from varying from 141 μm at the center to 1.48 μm at the edge. The pattern was made with 50% duty cycle (the chrome line width was set to half the line spacing.)

The accuracy of this difficult hologram was shown to be excellent. The interferogram and a gray scale plot of the measured wavefront phase are shown in Fig. 14. The diffracted wavefront shows ripples that are only 0.018λ rms and $\pm \lambda/20$ p-v. The accuracy of the writer is calculated from this data using the average period $T = 2.05 \mu\text{m}$. The rms accuracy of the hologram pattern δ is

$$\delta = \frac{T \cdot W_{rms}}{\lambda} = 0.058 \mu\text{m}$$

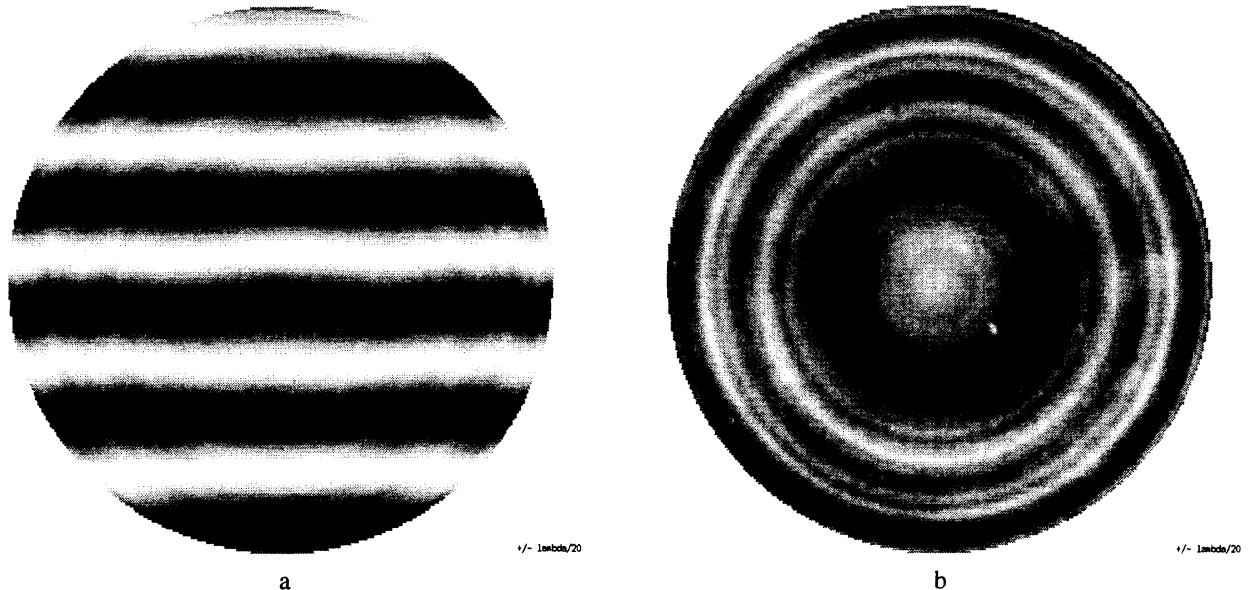


Figure 14. Measured wavefront from 58-mm $f/1.1$ zone plate from a phase-shifting Fizeau interferometer showing a) interferogram, and b) grey-scale phase map that uses shading to represent phase with full scale variation $\pm \lambda/20$.

A polarization test performed on this hologram showed no coupling between polarization and phase. The wavefront was measured using vertical linear polarization, then with horizontal polarization. The difference between the tests showed only about 2 nm of measurement noise.

The second example is a three-sector hologram for investigating of the methods for high numerical aperture (NA) hologram writing and verification of scalar theory of diffraction. The minimum hologram zone period T is defined as $T = \lambda/NA$. The holograms for testing of modern aspherical telescope mirrors¹⁵ should have $NA = 0.4 - 0.8$ and $0.8 - 1.3 \mu\text{m}$ zones period respectively. These sizes are commensurable with the wavelength and very difficult to fabricate, especially for the large holograms. One way to increase the zone period is to use higher orders of diffraction. By using the DOE in third order, the number of rings is reduced by a factor of three and the smallest feature size is increased by a factor of three. This makes the part much easier to fabricate. However, the applicability of the scalar theory for these holograms calculation is in question. The zone periods are nearly equal to the wavelength of the light, which clearly violates the assumption that the diffraction must be predicted by scalar diffraction theory. However, the experiment below demonstrates that the phase of the diffracted light does follow the scalar theory for these fast holograms.

For this preliminary investigation we fabricated the hologram (analog of a spherical mirror with radius of curvature Z) shown schematically in Fig.15a. The pattern was made with three sectors, using the first, second, and third diffracted order. The zone radii r_k in each hologram sector for order $n = 1, 2, 3$ can be expressed as

$$r_k = \sqrt{\frac{kn\lambda Z}{2} + \frac{k^2 n^2 \lambda^2}{16}}$$

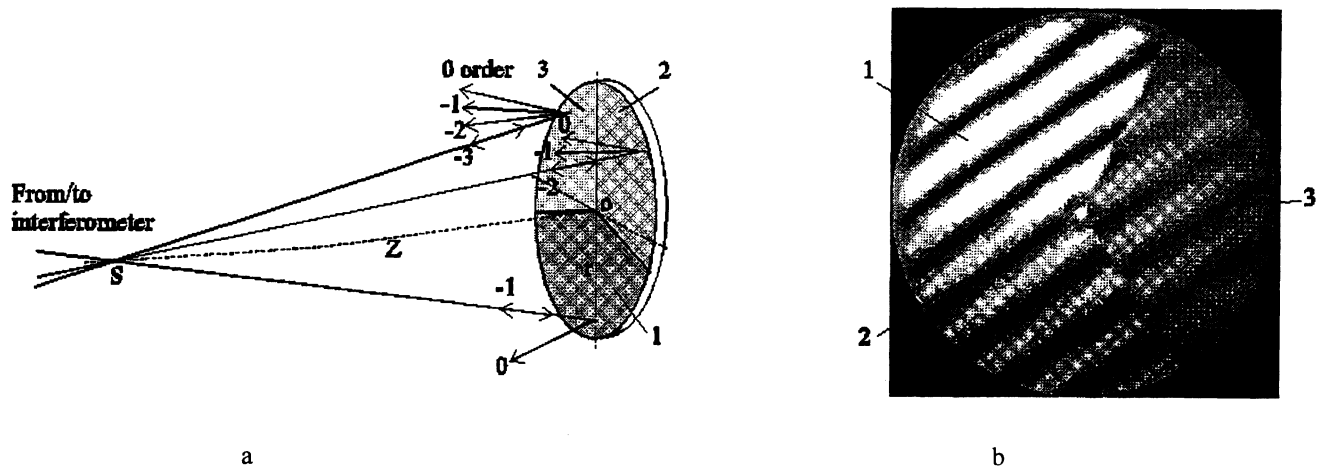


Figure 15. Optical diagram of three- sector hologram (a) layout and (b) interferogram of the diffracted wavefronts.

The hologram with $Z=25\text{mm}$ and diameter $D=10\text{mm}$ was fabricated and tested. The interferogram of the complex wavefront consisting of 1,2 and 3 diffractive orders is shown in Fig 15b. The diffraction efficiency of this amplitude hologram was about 10% for the 1st order (sector 1) and about 3% for the 3rd one (sector 3). This results in a large variation of the contrast between the different sectors (Fig.15b).

The zone plate was written using a $0.7\ \mu\text{m}$ diameter laser beam. Figure 16 shows microphotographs of the hologram zones in the central part (a) and at the sectors boundaries (b-d). The minimum zone period of $1.4\ \mu\text{m}$ is in sector 1 of the hologram. The overlapping displacement of the beam spot was 0 for writing $1.4\ \mu\text{m}$ zones (triple pass writing) and increased up to $0.5\ \mu\text{m}$ for the central large zones (see Fig.16a). The measurements for multiorders hologram have demonstrated that the wavefront distortions caused by writing and calculation errors are less than $\lambda/10$ for the zone periods of about 2λ , confirming the validity of scalar theory for the designs. The phase reversal for the third-order hologram is obvious in the interferogram.

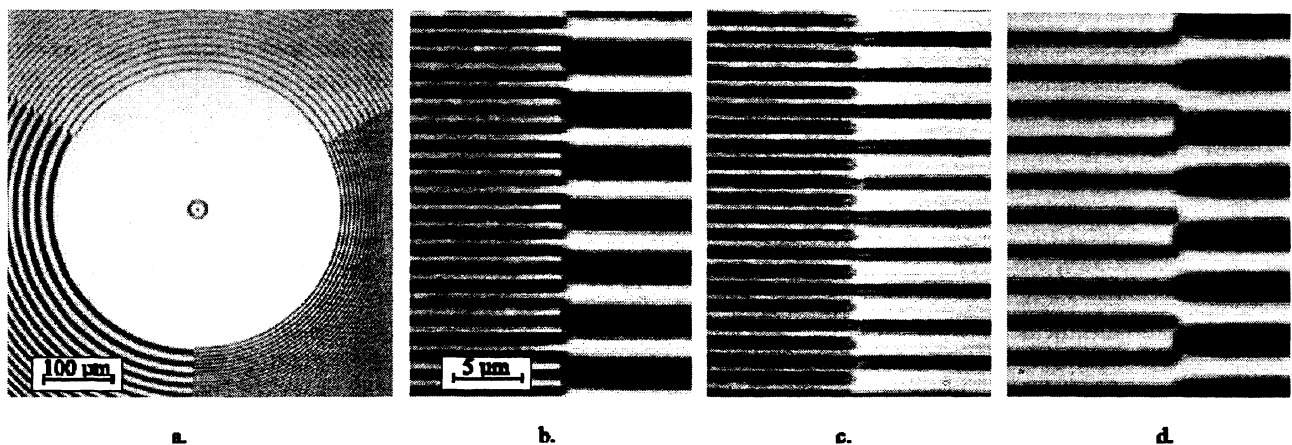


Figure 16. The microphotographs of the hologram zones in the central part (a) and at the sectors boundaries (b-d).

CONCLUSION

Large circular DOE's are optimally made using an accurate polar coordinate writing machine and the thermochemical recording process. The writing is shown to be tolerant of large power and velocity variations. The etching is shown to be insensitive to temperature and concentration variations. Large, fast patterns were fabricated using the methods described in this paper and the DOE's have been measured interferometrically and shown to have excellent accuracy.

REFERENCES

1. W. Goltsov, and S. Liu, "Polar coordinate laser writer for binary optics fabrication," Proc. SPIE **1211**, 137-147 (1990).
2. T. Nomura, K. Kamiya, *et al.*, "An instrument for manufacturing zone-plates by using a lathe," Precision Engineering **16**, 290-295 (1994).
3. S. Ogata, M. Tada, and M. Yoneda, "Electron-beam writing system and its application to large and high-density diffractive optic elements," Appl. Opt. **33**, 2032-2038 (1994).
4. V. P. Koronkevich, V. P. Kirianov, V. P. Korol'kov, A. G. Poleshchuk, V. V. Cherkashin, E. G. Churin, and A. M. Kharissov, "Fabrication of diffractive optical elements by direct laser writing with circular scanning," Proc. SPIE **2363**, 290-297 (1995).
5. V. P. Koronkevich, V. P. Kirianov, V. P. Kokoulin, I. G. Palchikova, A. G. Poleshchuk, A. G. Sedukhin, E. G. Churin, A. M. Sherbachenko, Yi. I. Yurlov, "Fabrication of kinoform optical elements," Optika **67**, No. 3, 257-266 (1984).
6. V. P. Vieko, G. A. Kotov, M. N. Libenson, and M. N. Nikitin, "Thermochemical action of laser radiation," Sov. Phys. -- Doklady **18** (1), 83-85 (1973).
7. G. N. Buynov, N. P. Larionov, A. V. Lukin, K. S. Mustafin, and R. A. Rafikov, "Holographic interferometric inspection of aspherical surfaces," *Optical Technology* **38**, 194-197 (1971).
8. Y. Ichioka and A. W. Lohmann, "Interferometric testing of large optical components with circular holograms," Appl. Opt. **11**, 2597-2602 (1972).
9. R. Mercier and S. Lowenthal, "Comparison of in-line carrier frequency holograms in aspheric testing," Opt. Comm. **33**, 251-256 (1980).
10. H. Tanigawa, K. Nakajima, and S. Matsuura, "Modified zone-plate interferometer for testing aspheric surfaces," Opt. Acta **27**, 1327-1334 (1980).
11. J. H. Burge, "Certification of null correctors for primary mirrors," Proc. SPIE **1994**, 248-259 (1993).
12. H. M. Martin, J. H. Burge, D. A. Ketelsen, and S. C. West, "Fabrication of the 6.5-m primary mirror for the Multiple Mirror Telescope Conversion," Proc SPIE **2871**, (1996).
13. J. H. Burge and D. S. Anderson, "Full-aperture interferometric test of convex secondary mirrors using holographic test plates," Proc. SPIE **2199**, 181-192 (1994).
14. J. H. Burge, "Measurement of large convex aspheres," Proc SPIE **2871**, (1996).
15. J. H. Burge, "A null test for null correctors: error analysis," Proc. SPIE **1993**, 86-97 (1993).
16. Koronkevich, V. P., A. G. Poleshchuk, E. G. Churin, and Yu. I. Yurlov, "Selective etching of laser exposure thin chrome films," Pis'ma v "Zhurnal tekhnicheskoi fiziki" (Letters to Journal of Technical Physics), v. 11 N 3, pp. 144-148 (1985).